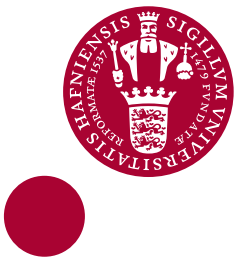

Electronic exitations of a single molecule contacted in a three-terminal configuration

Osorio, E.A.; O'Neill, K.; Wegewijs, M.; Stuhr-Hansen, Nicolai; Paaske, Jens; Bjørnholm, Thomas; van der Zant, S.J.

Published in:
Nano Letters

DOI:
10.1021/nl0715802

Publication date:
2007

Document version
Early version, also known as pre-print

Electronic excitations of a single-molecule transistor

Supplementary Information

Edgar A. Osorio,[1] Kevin O'Neill,[1] Maarten Wegewijs,[2] Nicolai Stuhr-Hansen,[3] Jens Paaske,[3] Thomas Bjørnholm[3*] and Herre S.J. van der Zant[1*]

[1] *Kavli Institute of Nanoscience, Delft University of Technology, PO Box 5046, 2600 GA, The Netherlands*
[2] *Institut für Theoretische Physik A, RWTH Aachen, 52056 Aachen, Germany*
[3] *Nano-Science Center (Department of Chemistry and Niels Bohr Institute), University of Copenhagen, Universitetsparken 5, DK-2100, Copenhagen, Denmark.*

Content:

[*]Email addresses: TB (tb@nano.ku.dk) and HvdZ (h.s.j.vanderzant@tudelft.nl).

1. Addition energies and excitations.

From Eq.2 in the main text we deduce the following energies for different *N*:

$$
\begin{aligned}
&E(0) = E_C(N_0 + N_G)^2 \\
&E(1) = E_C(1 - N_0 - N_G)^2 \\
&E'(1) = E_C(1 - N_0 - N_G)^2 + \delta \\
&E(2) = E_C(2 - N_0 - N_G)^2 + \delta - 3J/4 \\
&E'(2) = E_C(2 - N_0 - N_G)^2 + \delta + J/4 \\
&E''(2) = E_C(2 - N_0 - N_G)^2 + dU \\
&E'''(2) = E_C(2 - N_0 - N_G)^2 + 2\delta + dU \\
&E(3) = E_C(3 - N_0 - N_G)^2 + \delta + dU \\
&E'(3) = E_C(3 - N_0 - N_G)^2 + 2\delta + dU \\
&E(4) = E_C(4 - N_0 - N_G)^2 + 2\delta + 2\,dU
\end{aligned}
$$

with primed energies giving the excited configurations. Notice that for *N=+1, +3* all states are spin-doublets, whereas the lowest *N=+2* state is a singlet and the first excited state is a triplet. The highest excited states for *N=+2* are *intra*-orbital singlets. The electro-chemical potentials are found as $\mu(N) = E(N) - E(N-1)$:

$$
\begin{aligned}
&\mu(1) = E_C(1 - 2N_0 - 2N_G) \\
&\mu(2) = E_C(3 - 2N_0 - 2N_G) + \delta - 3J/4 \\
&\mu(3) = E_C(5 - 2N_0 - 2N_G) + dU + 3J/4 \\
&\mu(4) = E_C(7 - 2N_0 - 2N_G) + \delta + dU
\end{aligned}
$$

and the observable addition energies as $E_{add,N=+i} = \mu(i+1) - \mu(i)$:

$$
\begin{aligned}
&E_{add,N=+1} = 2E_C + \delta - 3J/4 \\
&E_{add,N=+2} = 2E_C - \delta + dU + 3J/2 \\
&E_{add,N=+3} = 2E_C + \delta - 3J/4
\end{aligned}
$$

Finally, the excitation energies for the different charge states are given by:

$$
\begin{aligned}
&ES^1_{N=+1} = \delta \\
&ES^1_{N=+2} = J \\
&ES^2_{N=+2} = dU - \delta + 3J/4 \\
&ES^3_{N=+2} = dU + \delta + 3J/4 \\
&ES^1_{N=+3} = \delta
\end{aligned}
$$

2. Negative Differential Resistance effect.

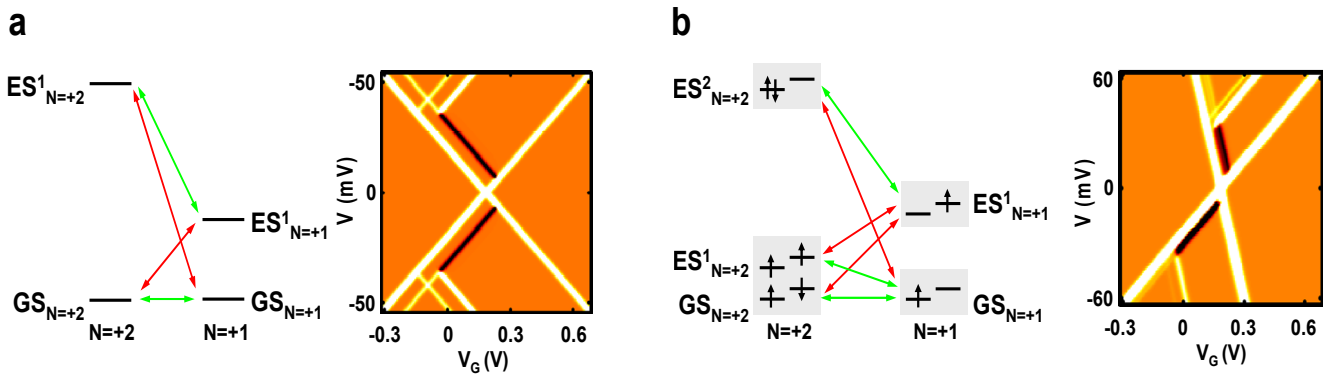

Figure 1S. ***a,*** *Schematic drawing of tunnelling transitions in a four-state model with symmetric gate coupling ($\alpha_+ = \alpha_-$ with $\alpha_+ = C_G/(C_G+C_D)$ and $\alpha_- = -C_G/C_S$) and* ***b,*** *in the full model from the main text (parameters are taken from the orbital filling model in section S1 and the gate couplings from the experimental calculated values), each with the corresponding dI/dV map. In* ***a*** *it is essential that all transitions indicated in red are slower by a factor 100 relative to the green transitions. The green E-E' transition is taken somewhat faster (1.5 times) than the G-G' one: this ensures that the NDR turns into a positive dI/dV at negative V_G for bias voltages >30 mV. In* ***b*** *the same relations hold between rates as in* ***a*** *for corresponding groups of states in the sketch. In addition, we incorporated a moderate reduction factor of 0.65 for transitions where an empty or doubly occupied orbital on the side of the electrode blocks the incoming hole / electron from that electrode. This causes the 30 meV excitation to appear only at V>0.*

The excitation exhibiting a sharp negative differential conductance is of special interest as it is drastically modified when another competing excitation becomes accessible at higher bias voltages at which point the NDR vanishes. This is a fingerprint of strong wave function-dependent tunnel processes (unrelated to spin or junction asymmetry), which are a marked feature of molecular three-terminal devices as demonstrated in this work. It is important to note that the NDR feature preserves its form for temperatures up to 11 K (stability diagrams for $T > 11$ K were not recorded), where temperature effects become important for the broadening of the resonances. At this temperature, and a sequential tunnelling picture starts to become applicable ($\Gamma \sim k_B T$). Furthermore, the picture of competing transport channels presented below is very robust and does not depend critically on the strength of the tunnel coupling Γ relative to T. The central point of this section is that the occurrence of NDR and the observation of transitions between two excited states (at 30 meV) indicate that relaxation processes are slower than any of the transport induced transitions.

The qualitative features of the data are readily reproduced in a simple sequential tunnelling model, presented in Fig. 1Sa, which we discuss first. The experimental transport fingerprint appears in such a model only when *i*) a minimum of four states is accounted for, a ground- (G,G') and excited (E,E') state in each of the two adjacent molecular charge states, and *ii)* the rate constants for transitions between excited and ground (G-E',G'-E) are much smaller than those for ground-ground (G-G') and excited-excited (E-E') transitions as sketched in Fig. 1Sa.

The NDR effect is most easily understood in a time-averaged picture: the fast G-G' and E-E' transitions or "channels" are responsible for transport and there are rare transitions in which the system switches from one channel to the other. If initially only the G-G' channel is open, NDR occurs if the slow transition G→ E' is switched on with increasing bias, while the E→E' transition is not yet energetically possible. This occurs for gate voltages close to the degeneracy point in Fig. 1Sa. The system spends a significant fraction of the transport cycle in the "closed channel" leading to a significant reduction of the current. In contrast, if the E↔E' channel is already open with the E→G' transition switched on, the current only changes slightly; the dark line changes into a white line as illustrated in the left upper and lower corners of the stability diagrams in Fig. 1Sa.

This simplified picture applies to the more complicated electronic spectrum inferred from the experimental data, if groups of relatively closely-spaced states take over the role of G, G, E, E' states. In Fig. 1Sb we incorporated all the electronic excitation energies as determined in the previous section and we fixed the relative magnitudes of the rate-constants analogous to the simple four state model. The gate coupling factors were taken from the experimental data. The model then reproduces nearly all the qualitative features of the data. When comparing, one should note that in the experiment a superposed background conductance (see Section 3) causes the NDR effect for $V<0$ to appear as a narrow $\mathrm{d}I/\mathrm{d}V$ plateau instead of a dip.

The microscopic origin of the strong state dependence of the tunnel rates cannot be inferred from the data. However, all transitions are spin-allowed ($\Delta S=1/2$) and the experimental data show no evidence of a very strong asymmetry between the tunnel rates associated with the left and right electrodes. *The NDR effect therefore indicates that the spatial structure of the many-particle ground and excited states are very dissimilar and that this difference is preserved upon charging the molecule*. Vibrationally assisted tunnelling may modify the sequential tunnelling rates and may contribute to the asymmetry pointed out here. A quantitative description of this lies beyond the scope and accuracy of the present work. Given the simplicity of the model, it is surprising that the particular choice of values for the rates in Fig. 1Sb leads to a good agreement with the experimental features, indicating that the model captures the basic underlying physics of the transport mechanism.

3. Effective model for $N = 2$: Finite-bias singlet-triplet Kondo effect

As demonstrated in the main text, the observed sequential tunnelling spectroscopy, including the NDR, is consistent with a simple model with two low-energy orbitals, *A* and *B*. If the charged molecule was stabilized by image-charge potentials due to the metallic electrodes, one would expect these orbitals to be localized near the two leads. Nevertheless, as argued in the main text, the reduced life-time broadening and the strong sensitivity to the back-gate potential for the *N=+2* charge state seems to indicate that the doubly charged molecule has the excess-charge localized more towards the middle of the molecule. Thus, the exact meaning of orbitals *A* and *B* cannot be the same in the different charge states *N=+1, +2*; if singly charged, the orbital *A* seems to be localized close to one of the leads. In the main text we argued that this observation is in fact consistent with well-known chemistry of an isolated OPV-5 molecule.

The most general situation in the *N=+2* charge state is sketched in Fig. 2S, depicting an effective two-orbital Anderson model in which the proximity to the leads is modelled by 4 different tunnelling-amplitudes. Transport will be feasible via either orbital *A* ($t_{SA}t_{AD}$) or *B* ($t_{SB}t_{BD}$), or via *AB* ($t_{SA}t_{AB}t_{BD}$ or $t_{SB}t_{BA}t_{AD}$), involving a weak *inter*-orbital tunnel coupling. The corresponding two-orbital Anderson model incorporating all five tunnel-couplings is tremendously rich (cf. e.g. Refs.[1-4]) but we shall restrict ourselves by drawing a few basic conclusions from perturbation theory.

The lowest lying states are well protected by a gap of roughly 35 meV up to the next excitation, comprised by many-body states with an entirely different charge-density profile. This is a remarkable separation of energy scales which is never found in traditional quantum dots, where the excitation energies are always much smaller. In our simplified model we can therefore safely leave out these high-lying states corresponding to two electrons in the same effective orbital when we want to describe merely the inelastic co-tunnelling below 2 meV. From the magnetic field dependence, the *N=+2* ground state was argued to be an inter-orbital spin-singlet and the excited state observed at ±1.7 meV to be a spin-triplet. In the middle of the *N=+2* diamond charge-fluctuations

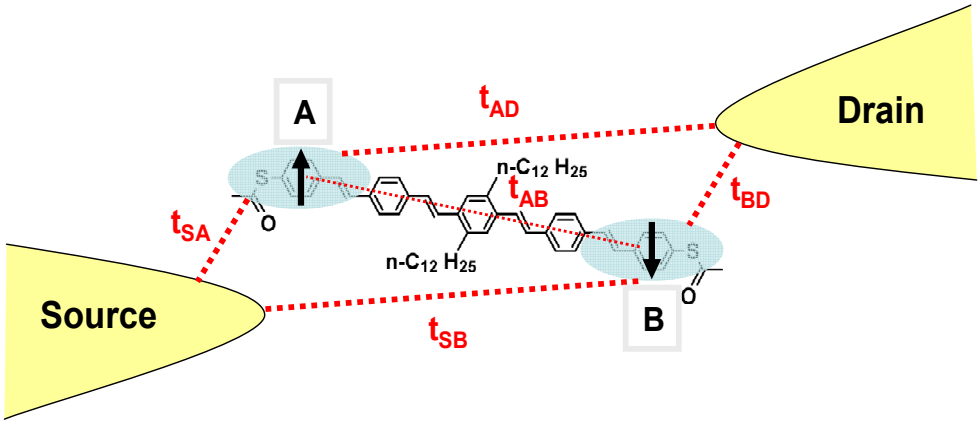

Figure 2S. Schematic drawing of the possible tunnel-couplings between the molecule and the source, drain electrodes. The blue shaded areas represent the orbitals A and B.

are strongly suppressed and virtual charge-fluctuations lead to an effective exchange coupling between the two spin-½ occupying the A,B-orbitals and the spins of the conduction electrons in the leads. Since our analysis of the addition energies shows that dU = 42 meV we include only the dominant virtual fluctuations in the N=+1 state, and omit fluctuations to the N=+3 state altogether. Performing this projection (*Schrieffer-Wolff* transformation) one arrives at the following effective *Kondo*-model:

$$H = \sum_{\substack{\vec{k},\sigma \\ \alpha=S,D}} (\varepsilon_{\vec{k}} - \mu_\alpha) c^\dagger_{\alpha\vec{k}\sigma} c_{\alpha\vec{k}\sigma} + J\,\vec{S}_A \cdot \vec{S}_B + H_{int}$$

with the antiferromagnetic exchange-coupling J = 1.7meV and the exchange-tunnelling terms

$$H_{int} = \sum_{\substack{\vec{k},\vec{k}';\sigma,\sigma' \\ \alpha,\alpha'=S,D \\ i=A,B}} J^i_{\alpha'\alpha} \vec{S}_i \cdot c^\dagger_{\alpha'\vec{k}'\sigma'} \vec{\tau}_{\sigma'\sigma} c_{\alpha\vec{k}\sigma} \ ,$$

Where $\vec{\tau}$ is the vector of Pauli matrices and where the couplings are given by $J^i_{\alpha'\alpha} = t^*_{i\alpha'} t_{i\alpha} / E_C$, assuming for now that $t_{AB} = 0$. The current carried by this exchange tunnelling will be an odd function of the applied bias-voltage and in the special case where all $t_{i\alpha}$ are equal the current will in fact vanish. This is seen by writing $\sum_{i=A,B} J^i_{\alpha'\alpha} \vec{S}_i = \sum_{i=+,-} J^i_{\alpha'\alpha} \vec{S}_i$ with $J^\pm_{\alpha'\alpha} = (J^A_{\alpha'\alpha} \pm J^B_{\alpha'\alpha})/2$ and $\vec{S}_\pm = \vec{S}_A \pm \vec{S}_B$ and using the singlet-triplet representation $\vec{S}_+ = \vec{S}$ and $\vec{S}_- = \vec{T}$ with:

$S^z = \lvert 1\rangle\langle 1\rvert - \lvert -1\rangle\langle -1\rvert$	$T^z = \lvert 0\rangle\langle s\rvert + \lvert s\rangle\langle 0\rvert$
$S^+ = (S^-)^\dagger = \sqrt{2}\left(\lvert 1\rangle\langle 0\rvert + \lvert 0\rangle\langle -1\rvert\right)$	$T^+ = (T^-)^\dagger = \sqrt{2}\left(-\lvert 1\rangle\langle s\rvert + \lvert s\rangle\langle -1\rvert\right)$

Since only $\vec{T}$ couples the singlet and the triplet-states there are no exchange tunnelling terms involving the singlet and therefore no current in the case of equal couplings. So, a finite current demands asymmetric couplings (the generic case) or an additional potential scattering term.

The antiferromagnetic exchange coupling J we ascribe to a super-exchange mechanism, which involves consecutive hops along the molecule. Including an *inter*-orbital tunnel coupling in our simple two-orbital model would of course alter the energy analysis in the main text slightly due to a weak mixing with (anti-)bonding states, but the dominant energy scales dU and E_C would hardly be influenced. A finite *inter*-orbital tunnelling also leads to new exchange-tunnelling terms in the effective low-energy Kondo-model and therefore opens an extra channel for transport. Instead of introducing bonding/anti-bonding states, we include the leading order corrections to the transport merely by going one order higher in the Schrieffer-Wolf transformation. This generates the additional term:

$$H_{int}^{AB} = \sum_{\substack{\vec{k},\vec{k}';\sigma,\sigma' \\ \alpha,\alpha'=S,D}} J_{\alpha'\alpha}^{BA} \left\{ \left[\vec{S}_A \cdot \vec{S}_B + 1/4 \right] \tau_{\sigma'\sigma}^0 + \left[\vec{S}_A + \vec{S}_B - 2i(\vec{S}_A \times \vec{S}_B) \right] \cdot \vec{\tau}_{\sigma'\sigma} \right\} c_{\alpha'\vec{k}'\sigma'}^{\dagger} c_{\alpha\vec{k}\sigma} + (A \leftrightarrow B),$$

and renormalizes the exchange-interaction to $J - 2\sum_{\alpha}(J_{\alpha\alpha}^{AB} + J_{\alpha\alpha}^{BA})$, with third order couplings $J_{\alpha'\alpha}^{ij} = t_{\alpha' i}^{*} t_{ij} t_{\alpha j} / E_C^2$, where $i, j \in \{A, B\}$ and $i \neq j$. In the singlet-triplet representation, the vector-product spin-operator, $-2i(\vec{S}_A \times \vec{S}_B) = \vec{\vec{T}}$, contains the following matrix elements:

$\widetilde{T}^{z} = -\lvert 0\rangle\langle s\rvert + \lvert s\rangle\langle 0\rvert$	$\widetilde{T}^{+} = (-\widetilde{T}^{-})^{\dagger} = \sqrt{2}\left(\lvert 1\rangle\langle s\rvert + \lvert s\rangle\langle -1\rvert\right)$

Since the vector-product is anti-symmetric in the orbital indices *A* and *B*, this term drops out when all $t_{i\alpha}$ are equal and again there will be no transitions to the triplet state. In this case only the potential scattering term gives rise to a finite (constant) conductance. Nevertheless, in the generic case with different $t_{i\alpha}$ the triplet-states will become populated at sufficiently large bias-voltage and an inelastic co-tunnelling-channel opens up at e*V* = *J*.

We note that the present problem is different from that of a carbon-nanotube quantum-dot at an even charging-state, which also exhibits a finite-bias singlet-triplet conductance peak (cf. Ref.[4]). In contrast to the OPV5-molecule, the electrons in a nanotube are delocalised, the exchange coupling is very small and ferromagnetic (Hund's rule), the ground-state is an *intra*-orbital (sub-band) spin-singlet and the lowest excitations comprise an *inter*-orbital spin-triplet, thus giving rise to a conductance peak at voltage equal to the orbital splitting. In the generic case of different $t_{i\alpha}$ the differential conductance of the nanotube-system is asymmetric in the bias voltage *V*, consistent with the experiment analysed in Ref.[4]. In the present problem, however, the inter-orbital nature of the singlet ground state implies a conductance which is symmetric in bias-voltage, unless t_{AB} is different from zero. Thus the assumption of a *weak* inter-orbital tunnelling strength is consistent with the relatively weak asymmetry of the differential conductance measured in the *N*=+*2* charge state (cf. Fig. 3S).

The zero-bias peak observed in the middle of the *N*=+*1* Coulomb-blockade diamond (cf. Fig. 3a in the main text) exhibits an unusual skewed line-shape at variance with the expectation for the Kondo-resonance of a singly occupied orbital. A similar skewness is observed in the *N*=+*2* data (cf. Fig. 3S), and while it is difficult to ascertain the exact physical origin of this asymmetry the data do in fact exhibit an extra feature which points to a second molecule in parallel playing a role. That is, defining a background conductance by what must be subtracted to make the *N*=+*1* peak in Fig. 3a of the main text symmetric, we note that a subtraction of that same background in the *N*=+*2* diamond makes those data nearly symmetric as well. In Fig. 3S we show a set of *dI/dV* curves for different gate-voltages in the *N*=+*2* diamond before and after subtraction. Clearly the middle curve in the right panel, corresponding to gate-voltage in the middle of the *N*=+*2* diamond, is almost perfectly symmetric. How exactly a molecule in

parallel leads to an asymmetric background is not clear to us at this point, but one possible explanation could be an effective *band-filtering* (cf. Fig.4f in Ref.[5]).

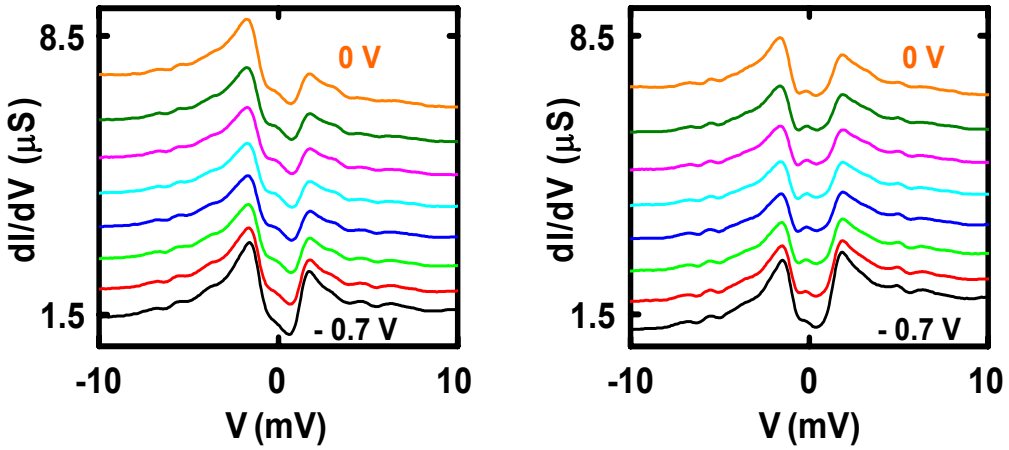

Figure 3S. Traces of the differential conductance, dI/dV, for different gate-voltages in the N=+2 Coulomb-blockade diamond, before (left) and after (right panel) subtracting an asymmetric background deduced from symmetrising the zero-bias peak observed in the middle of the N=+1 diamond. Curves were offset for clarity and taken at gate voltages from –0.7 to 0 V in steps of 0.1 V.

Interestingly, this background subtraction also emphasizes another feature of the data: a weak but clearly visible zero-bias anomaly. There is no source of zero-bias anomalies in our effective double-dot Hamiltonian, but a possible explanation could involve one of the low-lying vibrational modes. In the co-tunnelling regime we observe a number of vibrational modes at frequencies, which depend slightly on the charge state of the molecule. In the *N=+1* data we observe a mode very close to 1.7 meV and assuming that this mode is also present in the *N=+2* state, this could restore a zero-bias conductance anomaly involving the simultaneous transition from singlet to triplet and the absorption of a vibrational quantum, - a novel transport mechanism put forth in a recent paper by Kikoin *et al*. [6].

The *N*=+2 data could in principle be fitted in the same manner as was done for the carbon nanotube in Ref.[4], to quantify the relative strength of the Kondo-correlations and non-equilibrium effects involved in the conductance peaks near $V = \pm J$. The Hamiltonian is slightly different, but the renormalization group equations look similar and the rest of the calculation proceeds exactly as described there. However, since we cannot fully determine the influence from the background we choose not to present any quantitative fit to these data. *Qualitatively*, we observe well-developed peaks of width comparable to *J* and a rounded "valley" for voltages smaller than *J*, which indicates a marked influence of both Kondo-correlations and non-equilibrium effects (cf. Ref. [4]).

4. Stability diagram after transferring the probe to a different dewar.

To perform measurements in a magnetic field, the ^{4}He insert had to be transferred from one dewar to another. After transfer, we have measured the dI/dV map once again using the same parameters as before. The result is shown in Fig. 4Sb. The striking observation is that the degeneracy point on the far left has moved to a more positive gate voltage whereas all other features remained the same. This observation indicates that the degeneracy point on the left belongs to a different molecule in parallel. The shift in gate voltage can be explained by a change in its electrostatic environment, probably because the molecule has moved. In contrast, the molecule of which the features are discussed in the main paper has not moved; all details including the singlet-triplet co-tunnelling, the addition energies and the excitations are unaltered.

Note that the temperature dependent measurements presented in Fig. 3 of the main text were performed before the sample was transferred into the dewar with the magnet.

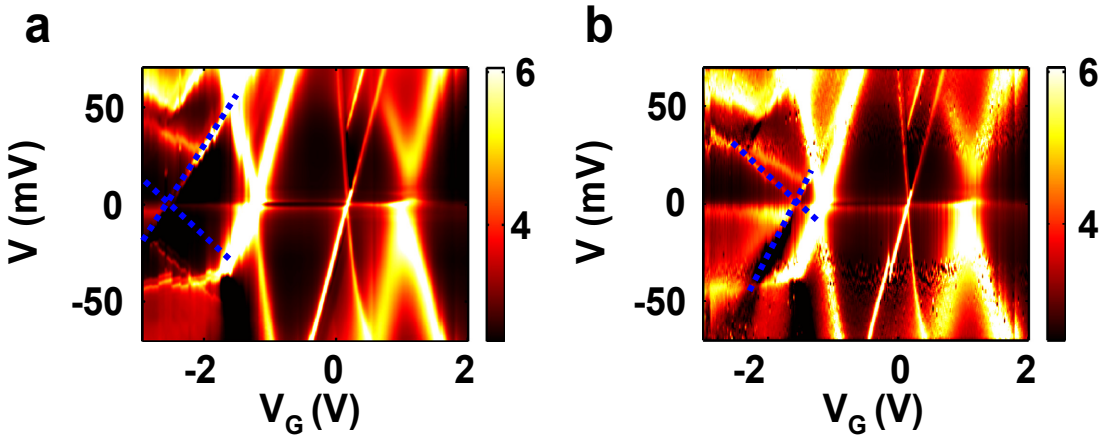

Figure 4S. Two-dimensional colour plot of the differential conductance, dI/dV, versus V and V_G at T = 1.7 K. ***a,*** *Before the sample was transferred.* ***b,*** *After transfer into a different dewar in which magnetic field measurements could be performed. Dashed lines indicate the diamond edges of the second molecule in both plots.*

References:

[1] Meden, V., Marquardt, F. Correlation-Induced Resonances in Transport through Coupled Quantum Dots, *Phys. Rev. Lett.* **96**, 146801 (2006).
[2] Kashcheyevs, V., Schiller, A., Aharony, A., Entin-Wohlman, O. Unified description of correlations in double quantum dots. *cond-mat/0610194*.
[3] Zarand, G., Chung, C.-H., Simon, P., Vojta, M. Quantum criticality in a double quantum-dot system. *cond-mat/0607255*.
[4] Paaske, J., Rosch, A., Wölfle, P., Mason, N., Marcus, C.M., Nygård, J. Non-equilibrium singlet-triplet Kondo effect in carbon nanotubes. *Nature Physics* **2**, 460 (2006) [Supplementary Information].
[5] Dias da Silva, L. G. G. V., Sandler, N. P., Ingersent, K., Ulloa, S. E. Zero-field Kondo splitting and quantum-critical transition in double quantum dots. *Phys. Rev. Lett.* **97**, 096603 (2006).
[6] Kikoin, K., Kiselev M.N., Wegewijs M.R. Vibration-induced Kondo Tunneling through Metal-Organic Complexes with Even Electron Occupation Number. *Phys. Rev. Lett.* **96**, 176801 (2006).